NAG1-635

IN-02
64835
CR
P. 25

Semi-Annual Status Report on NASA Grant NAG 1-635

"CALCULATION OF AERODYNAMIC CHARACTERISTICS AT HIGH ANGLES OF ATTACK FOR AIRPLANE CONFIGURATIONS

August 1, 1986 - January 31, 1987

by

C. Edward Lan and J.B. Tseng

Flight Research Laboratory

The University of Kansas Center for Research, Inc.

Lawrence, Kansas 66045

February 24, 1987

(NASA-CR-180678) CALCULATION OF AERODYNAMIC CHARACTERISTICS AT HIGH ANGLES OF ATTACK FOR AIRPLANE CONFIGURATIONS Semiannual Status Report, 1 Aug. 1986 - 31 Jan. 1987 (Kansas Univ. Center for Research) 25 p Avail: G3/02

N87-26860

Unclas
0064835

During this reporting period (August 1, 1986 to January 31, 1987), effort was directed to two tasks, namely;

- modeling airplane configurations;

- predicting nonlinear sectional characteristics.

Work accomplished during this period is presented below.

(1) Modeling airplane configurations

The primary objective of this project is to determine how an airplane configuration should be modeled to predict both longitudinal and lateral aerodynamic characteristics at high angles of attack. For this purpose the following configurations have been investigated: A generic fighter model, an F-16 and an F-18 configuration with leading-edge flap deflection and an F-106B configuration. Furthermore, the F-16XL and X-29 configurations have also been examined. Calculated results for the latter configurations will be presented in the final report. In the following, some calculated results will be presented and discussed.

(a) Modeling a generic fighter configuration.

This is an airplane model tested in the 12-ft tunnel at NASA Langley Research Center (Ref. 1). As shown in Fig. 1, the configuration includes a cylindrical body with lifting and control surface made of flat plate. The sectional data from Ref. 2 were used in the calculation . The nonlinear sectional data were used as near-field solutions to be matched iteratively with far-field solutions obtained from a lifting-surface theory. In the calculation an over relaxation factor was used for the wing. However, the horizontal tail required an underrelaxation factor to achieve convergence. This is probably mainly due to a coplanar wing-tail interaction. In this case, not only the vortex strips on the wing and tail must be lined up to avoid unrealistic downwash induced on the tail, but also the relaxation factor on the tail must be reduced to avoid divergence. Figs 3 and 4 show the predicted results. It is seen that at angles of attack greater than 22 deg., the lateral characteristics are not correctly predicted. This is probably due to forebody vortices which are not accounted for in the code.

(b) An F-16 configuration.

As shown in Fig. 5, this airplane has a slender leading-edge extension. Thus, an additional discrete strake vortex is needed to model the augmented vortex lift effect. Like other airplanes which have been modeled, there is no difficulty in modeling lifting surfaces. However, the F-16 has a distinct inlet which makes the body cross sections change rapidly. In addition the inlet makes it more difficult for the fuselage aerodynamic characteristics to cconverge if the real body shape with the nacelle is used. In the following, smooth body cross sections are assumed. The predicted over-all

characteristics, as shown in Figs 7 and 8, agree reasonably well with the experimental data.

(c) An F-18 configuration with deflection of leading edge flaps.

Calculation related to the F-18 in clean wing configuration has been reported in the last progress report. In this reporting period, effort was devoted to modeling the leading edge flap deflection. The deflected leading edge flaps tend to make the flow separate at a higher angle of attack. The 2-D viscous effect is accounted for by using nonlinear sectional data. The sectional characteristics used are shown in Fig. 10. Again, agreement between the calculated results and the experimental data is reasonable as can be seen in Figs. 11 and 12. The experimental data are taken from Ref. 3.

(d) An F-106 B configuration.

An attempt was made several years ago to predict lateral-directional characteristics of F-106B configurations with and without vortex flaps and compare these with data from the Langley 12-ft. tunnel. At that time, it was found that the predicted angle of attack for vortex breakdown to occur at the trailing edge was reasonable. However, the forward progression rate of burst point was predicted to be too fast, so as to cause inaccurate prediction of lateral characteristics at high angles of attack. The progression rate used in the code was based on data of thin flat delta wings. Recently, it was discovered that negative upper surface slopes in the spanwise direction due to thickness distribution tended to slow down the forward movement of burst point (see Fig. 13 and Ref. 4). After several exploratory numerical experimentation, it was found that if the spanwise upper surface angle (i.e., $\tan^{-1}(\partial z_c/\partial y)$) was assumed to reduce the local angle of attack to an effective value, the latter could be used to determine the delayed breakdown point location. Based on this idea, the F-106 configuration with the basic case 29 conical camber was re-examined. The results shown in Figs 14-15 now exhibit good agreement with data. Apparently, additional basic data on the effect of spanwise upper surface slope on vortex breakdown are needed.

(2) Predicting nonlinear sectional data

The airfoil codes being used are the Eppler's code and the SAAP code. Both codes can be used to determine the angle of zero lift and aerodynamic characteristics up to stall α. For a thin airfoil, the characteristics at angles beyond stall can not be predicted accurately by these airfoil codes. For the present purpose, they are assumed to follow the same shapes as a flat plate. The latter experimental characteristics can be found in Ref. 2. As an example, the c_ℓ vs α curve for an NACA 64A204 airfoil is illustrated in Fig. 6. For a thick wing, the Epplers code can be applied to obtain the 2-D characteristics. However, compared with the experimental data, the code

tends to overpredict the maximum lift coefficient. More research is needed to improve the theoretical method for stall and post-stall prediction of airfoil characteristics.

References

1. Nguyen, L.T., Whipple, R.D. and Brandon, J.M., "Recent Experiments of Unsteady Aerodynamic Effects on Aircraft Flight Dynamics at High Angle of Attack," AGARD CP-386, 1985.

2. Wick, B.H., "Study of the Subsonic Forces and Moments on an Inclined Plate of Infinite Span," NACA TN-3221, 1954.

3. Lutze, F.H., "Curved Flow Wind Tunnel Test of F 18 Aircraft," VPI-Aero-108, April 1980.

4. Earnshaw, P.B., "Measurements of the Effects of Thickness on Vortex Breakdown Position on a Series of Sharp-Edged Delta Wings," British ARC C.P. No. 1018, 1968.

5. Nguyen, L.T., Ogburn, M.E., Gilbert, W.P., Kibler, K.S., Brown, P.W. and Deal, P.L., "Simulator Study of Stall/Post-Stall Characteristics of a Fighter Airplane With Relaxed Longitudinal Static Stability," NASA TP-1538, Dec. 1979.

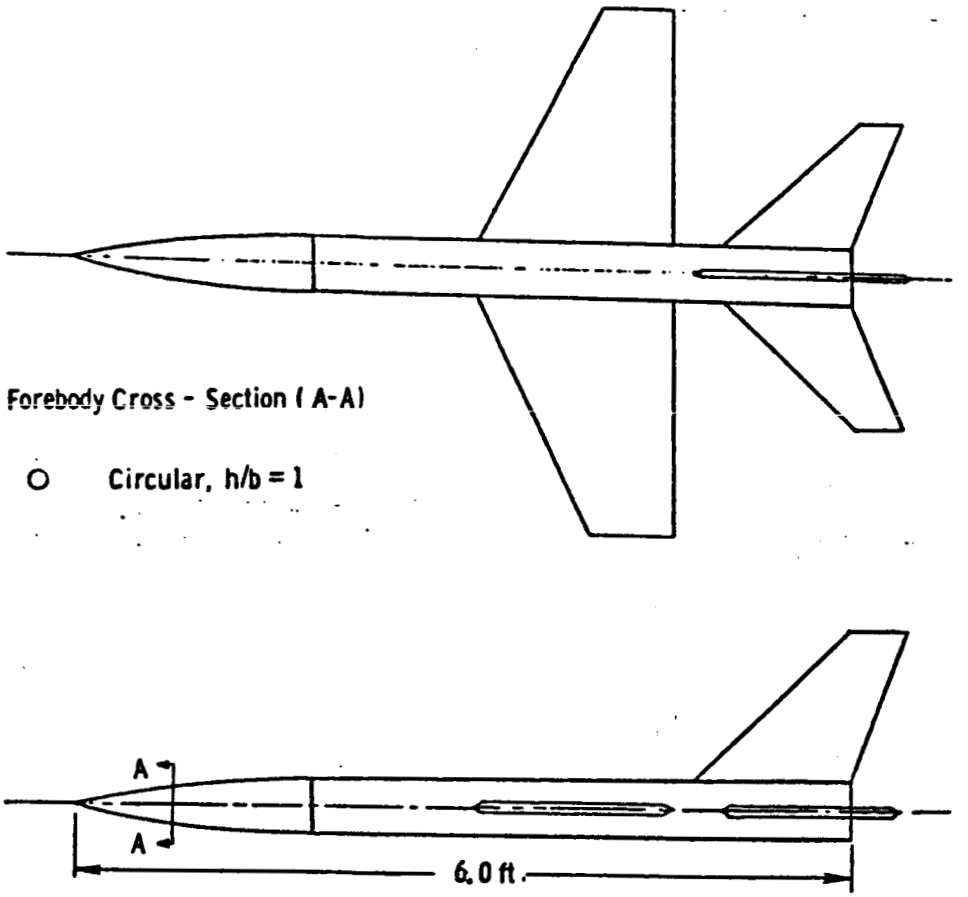

Figure 1. A Generic Fighter Model

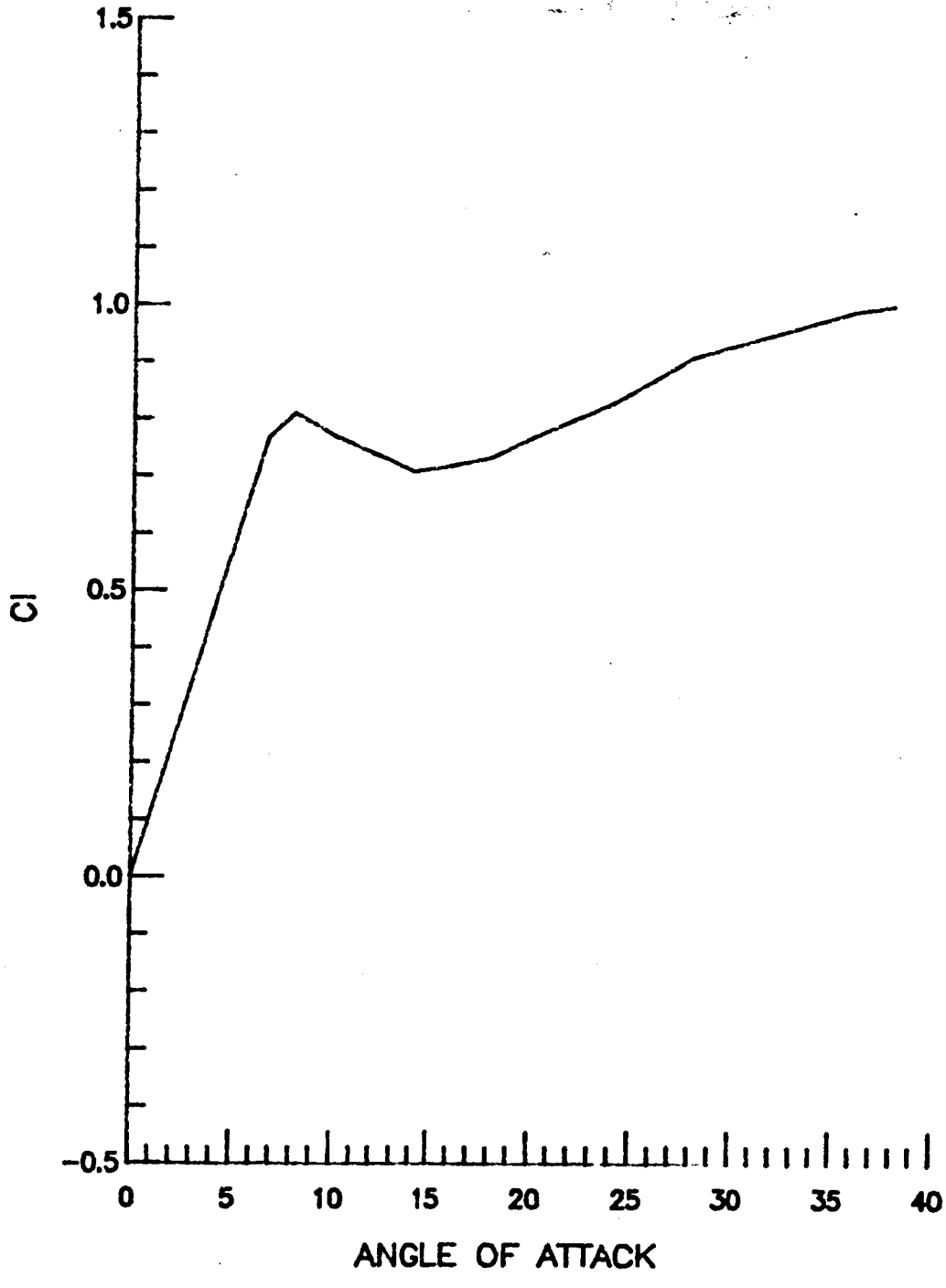

Figure 2. Lift Curve for a Flat Plate Airfoil

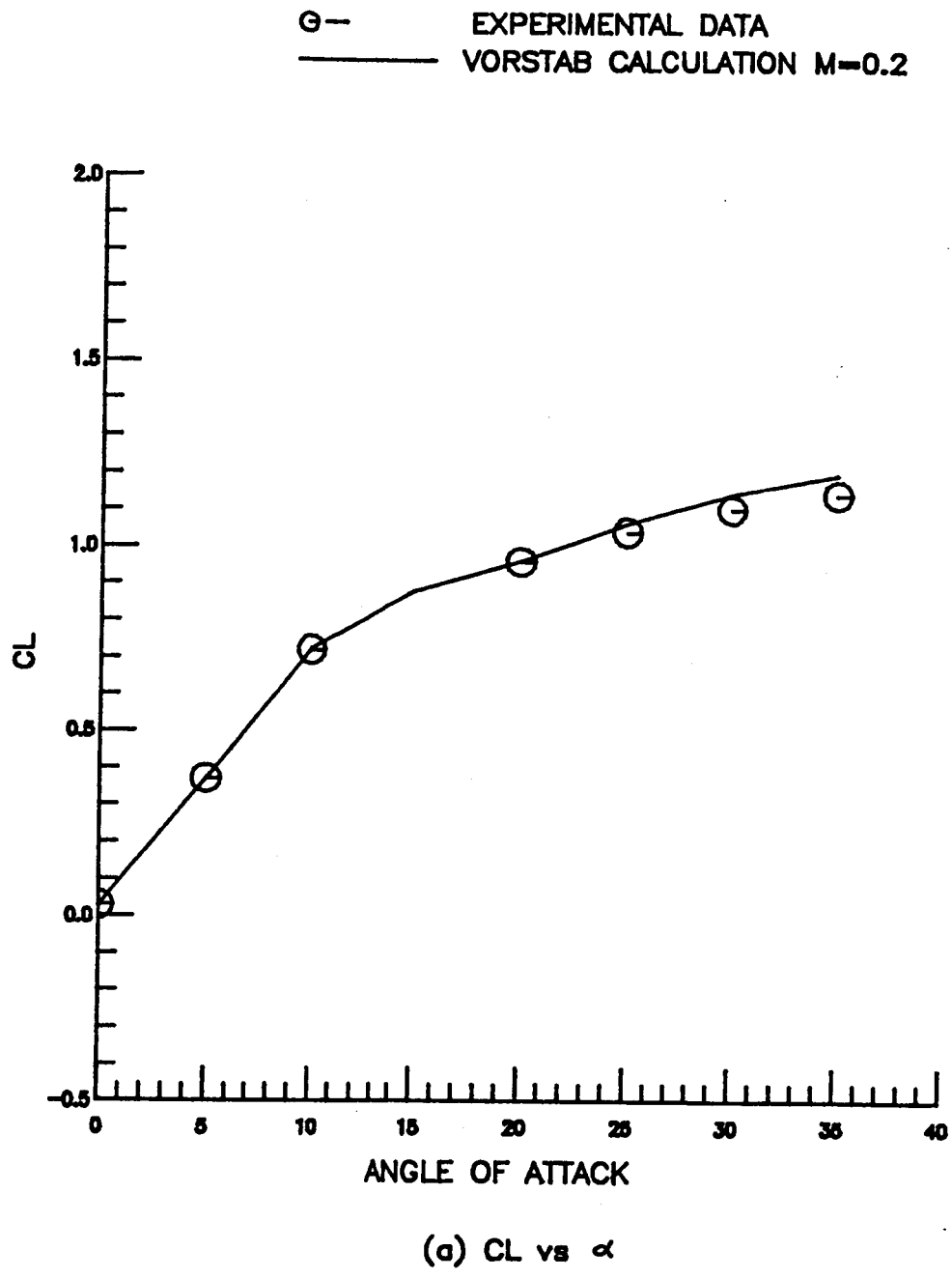

(a) CL vs α

Figure 3 Longitudinal Aerodynamic Characteristics for the Configuration of Figure 1.

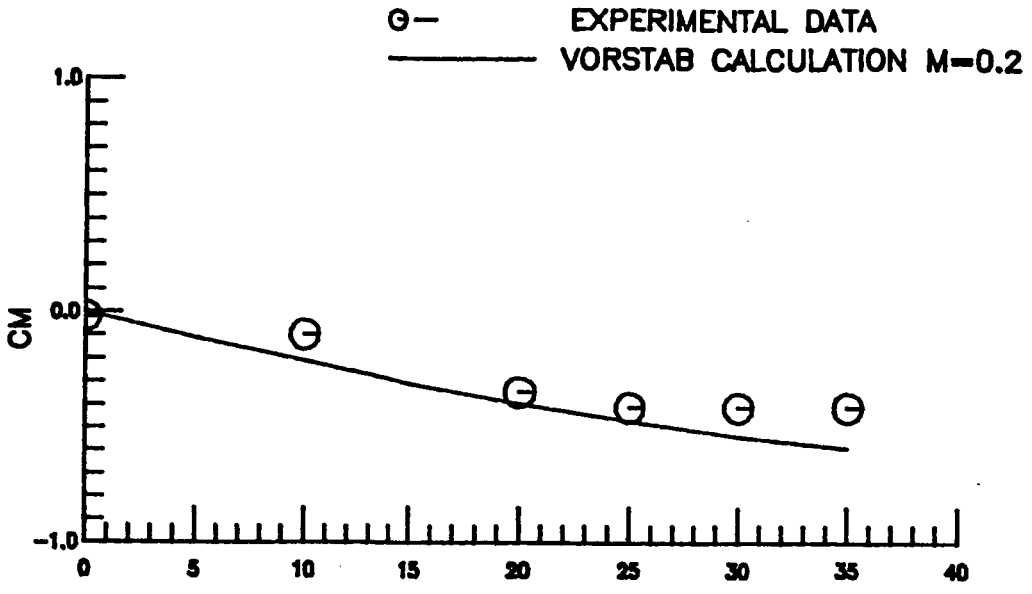

(b) CM vs α

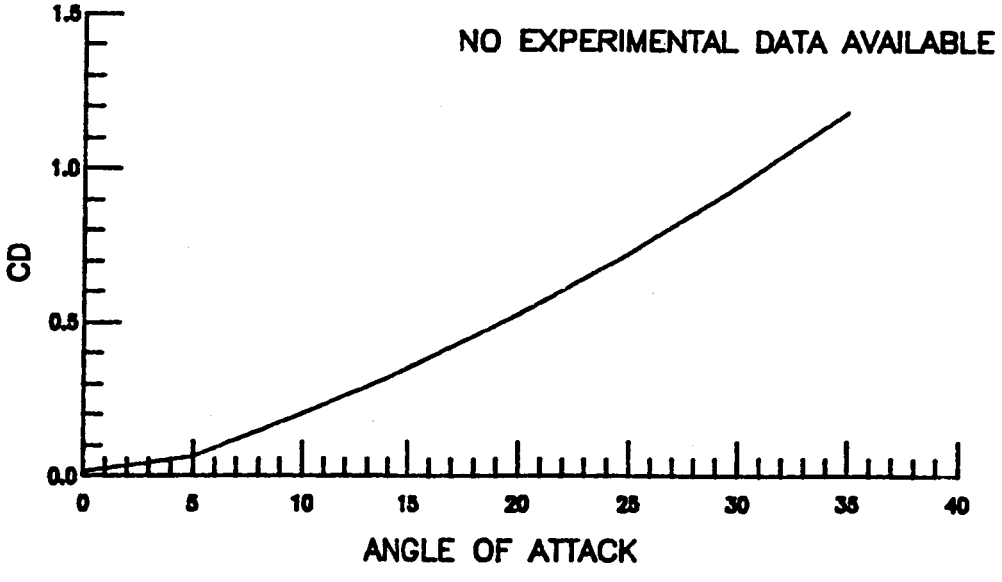

(c) CD vs α

Figure 3. Continued

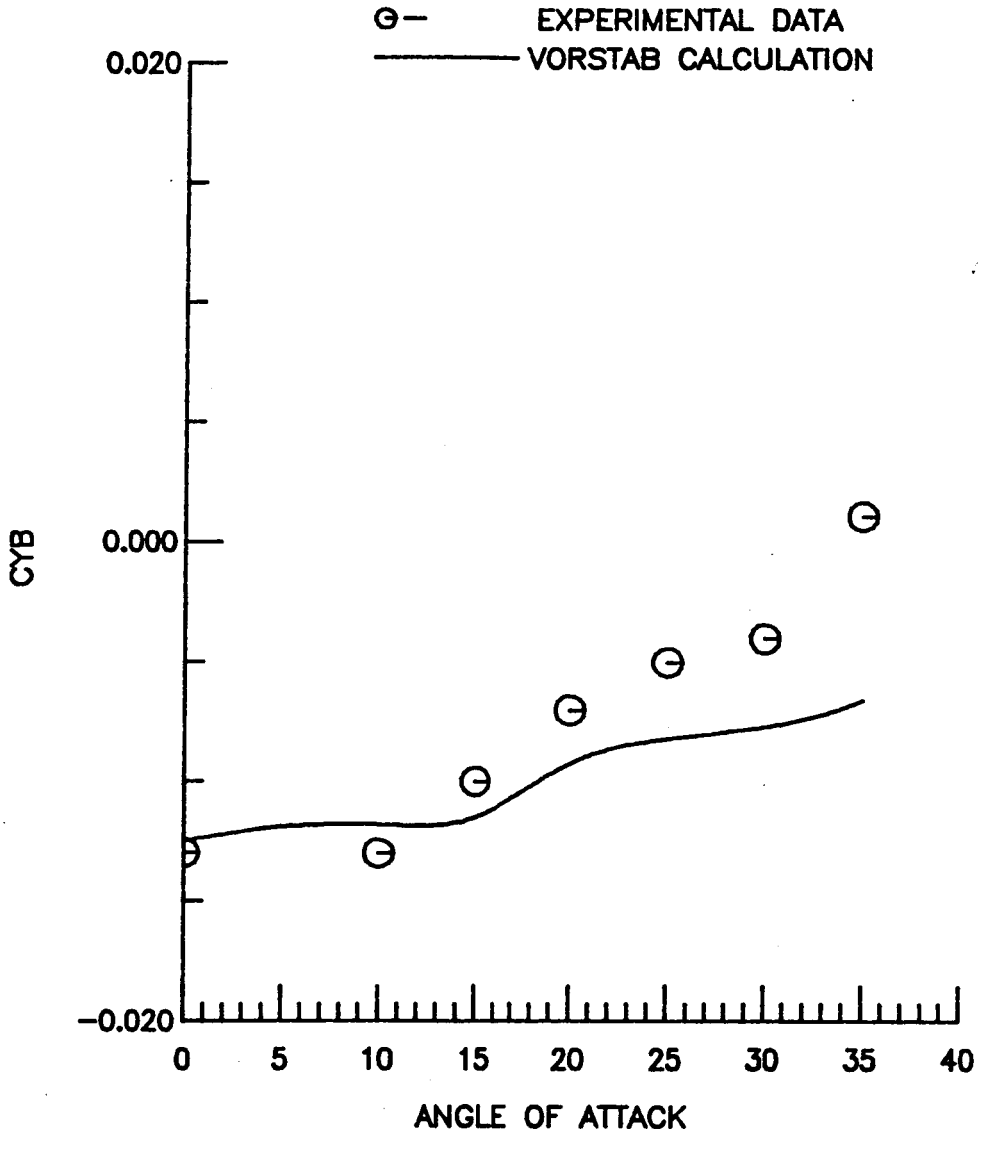

FIGURE 4. LAT—DIR DERIVATIVES CALCULATION BASED ON BODY AXIS AT β = 4 DEG.
For the Configuration of Figure 1.

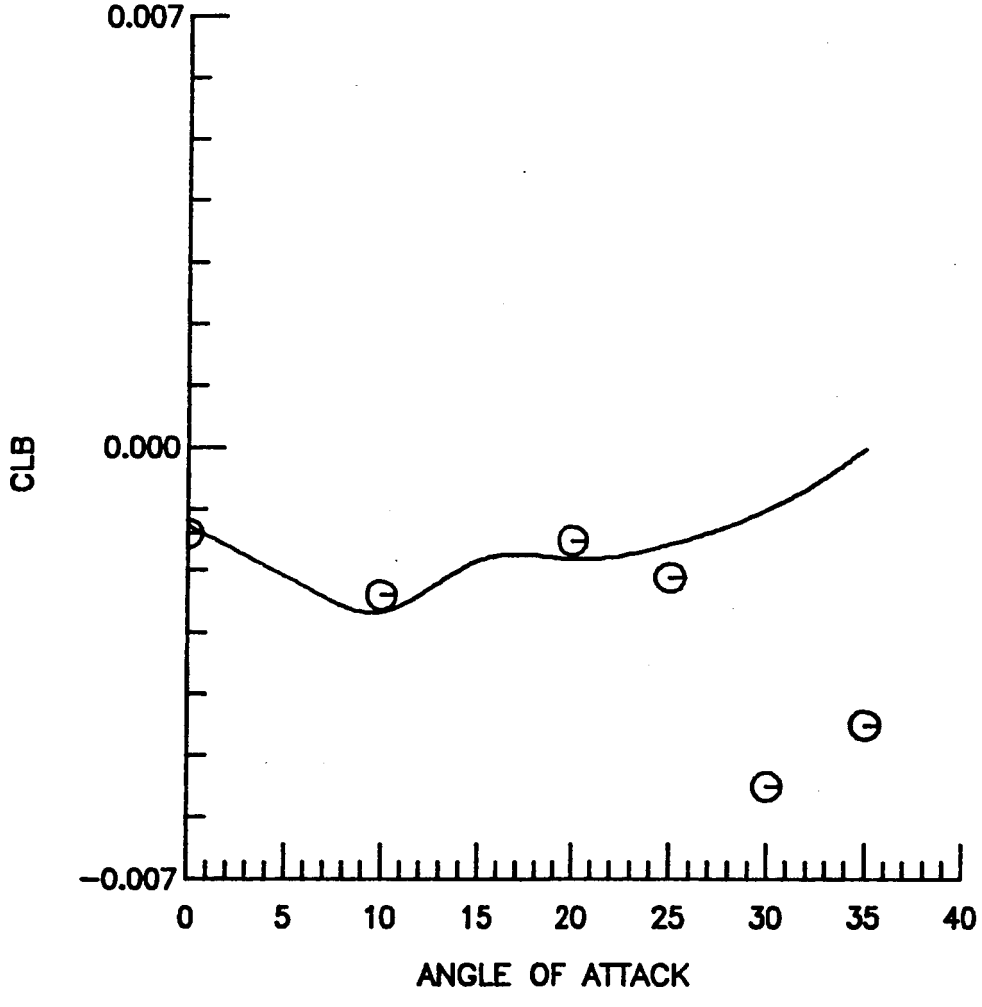

Figure 4. Continued

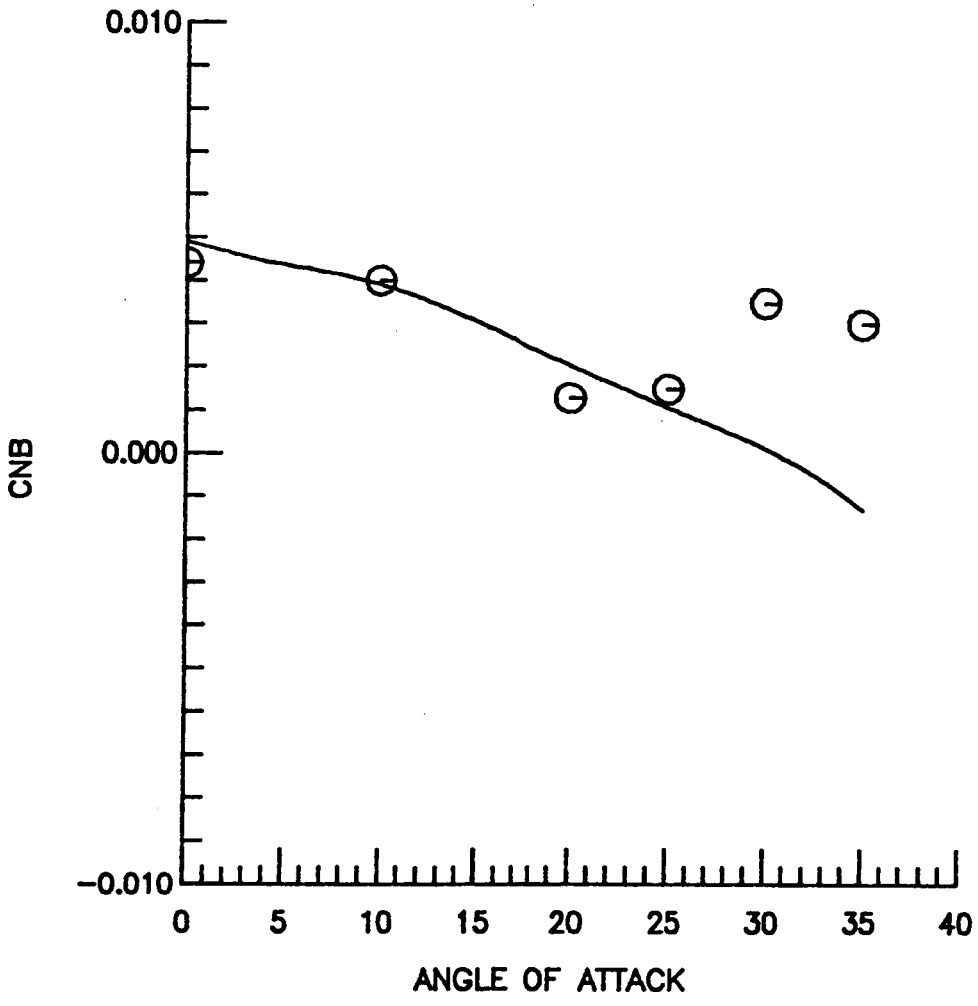

Figure 4. Continued

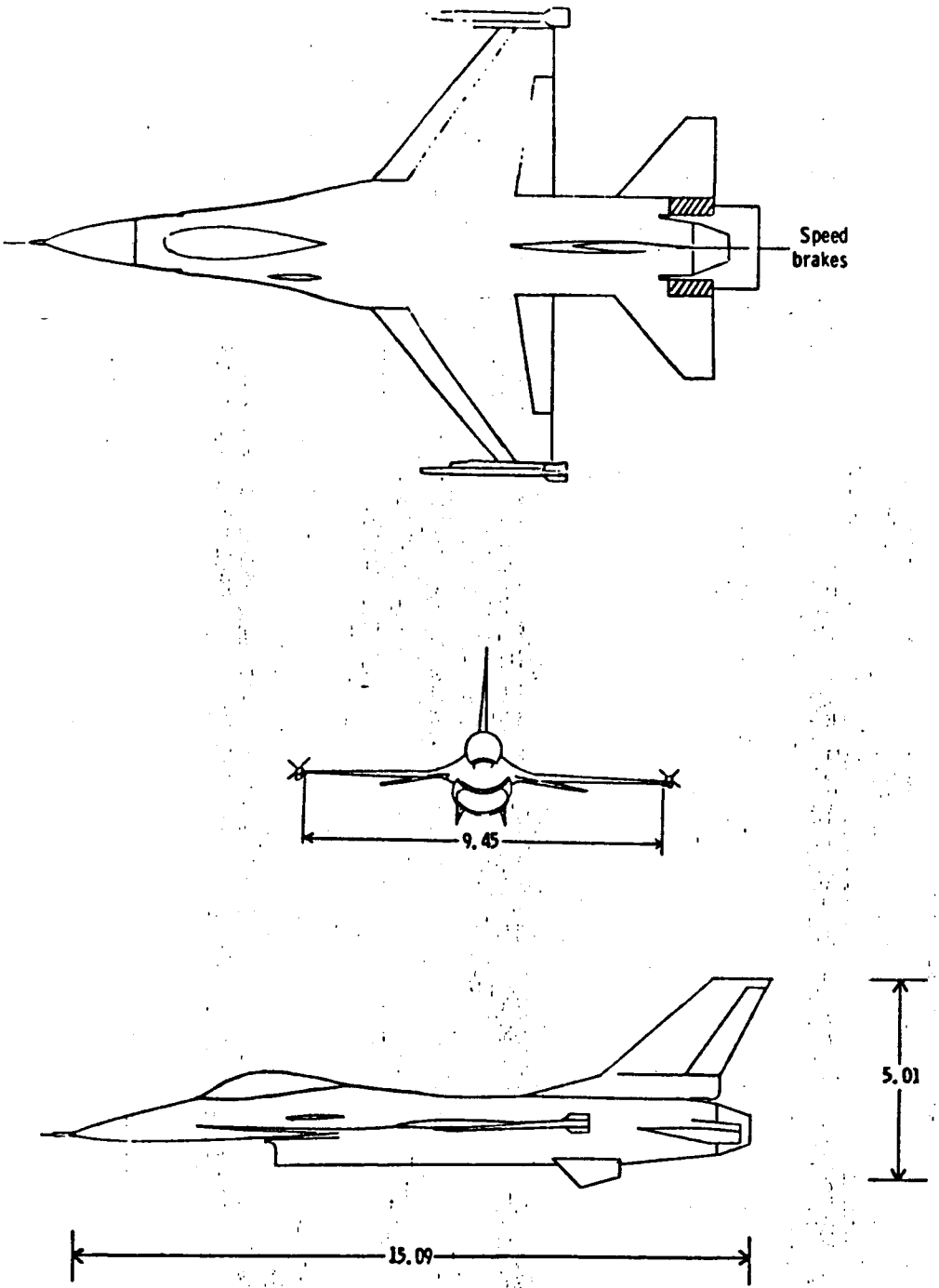

Figure 5. Three-view sketch of airplane configuration. All dimensions given in meters.

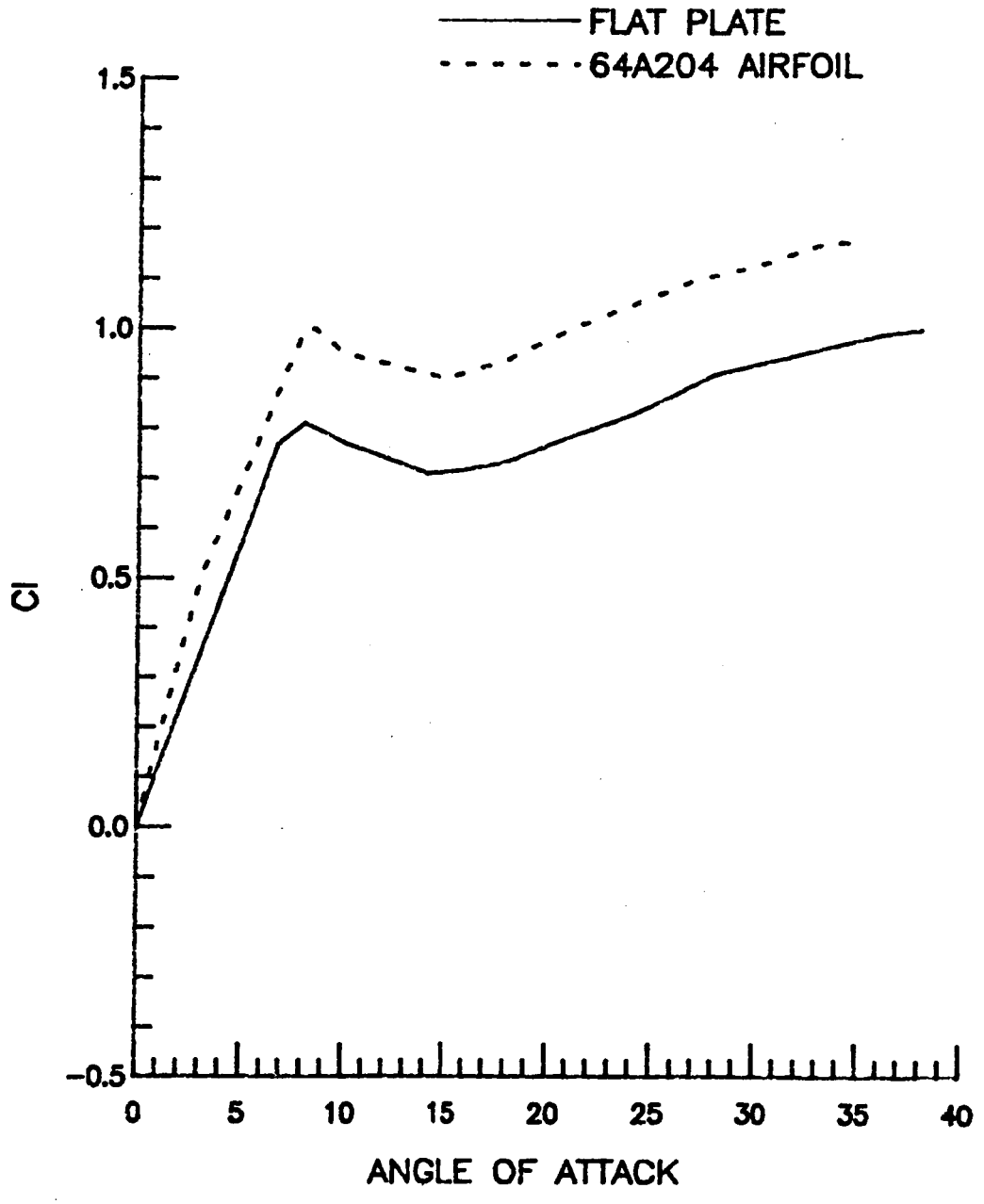

Figure 6. Lift Curve for a 64A204 Airfoil

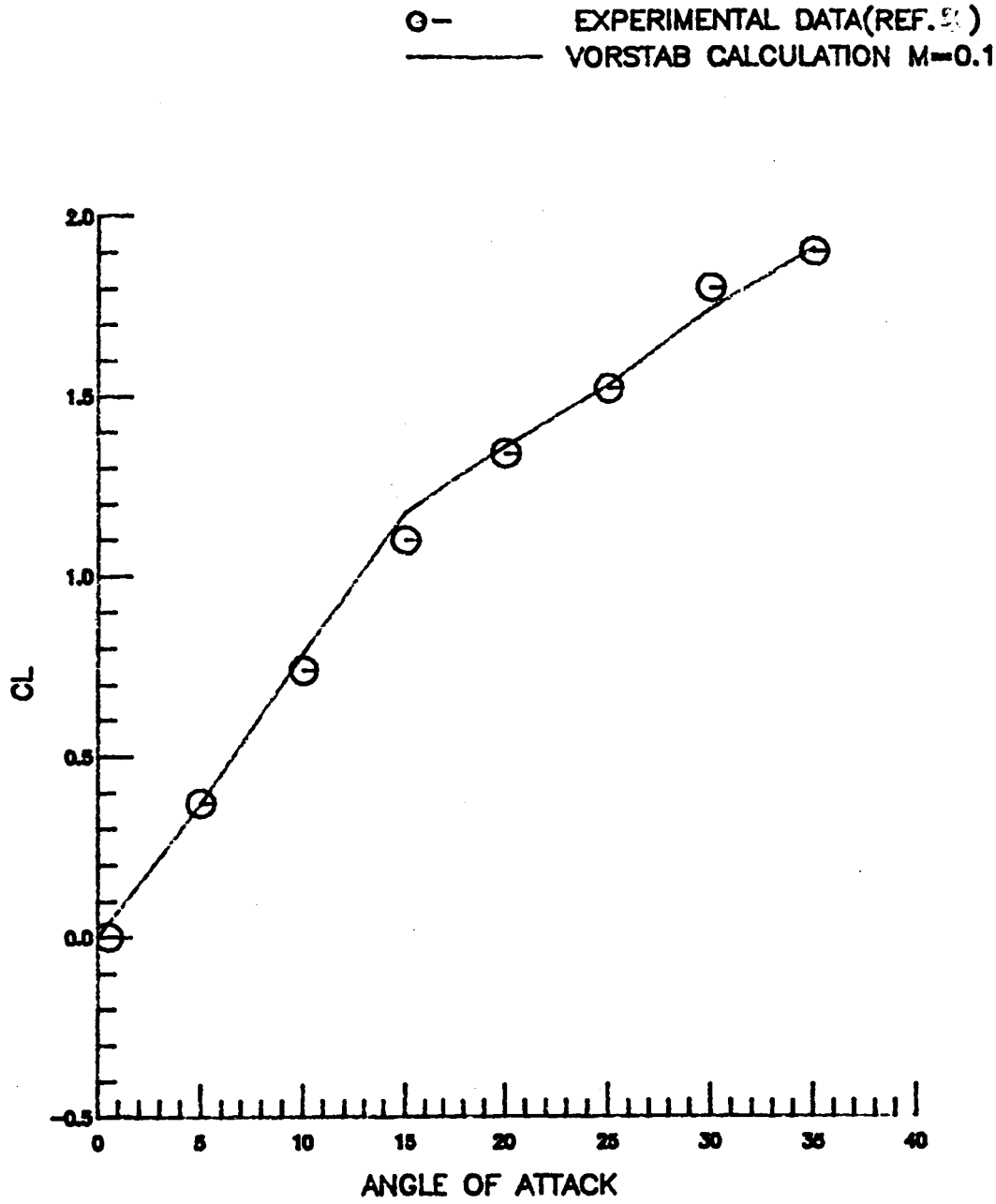

(a) CL vs

Figure 7. Longitudinal Aerodynamic Characteristics for a F-16 Configuration

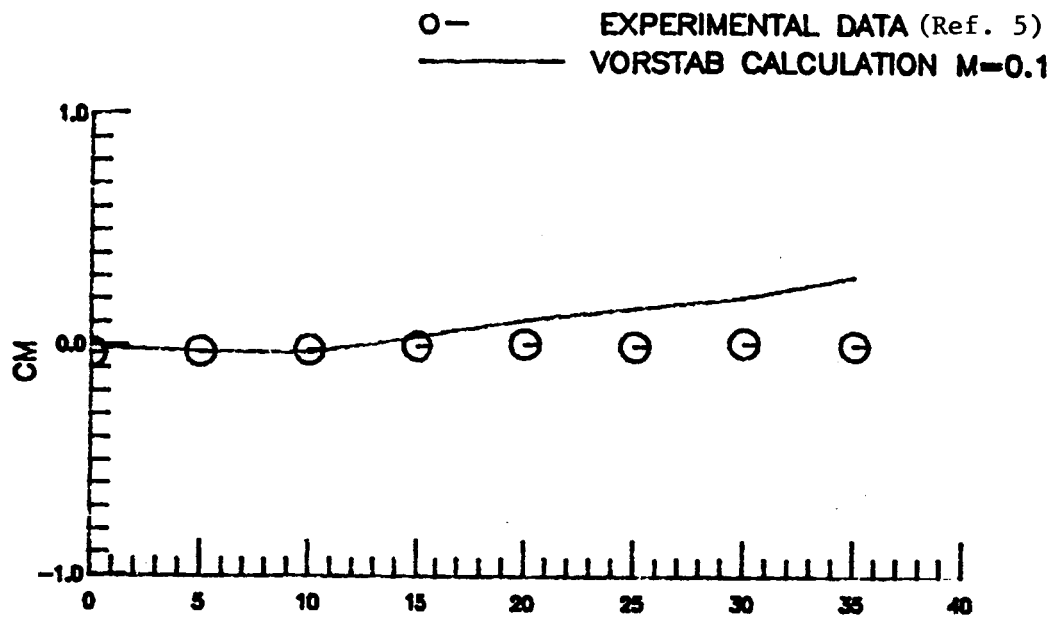

(b) CM vs

NO EXPERIMENTAL DATA AVAILABLE

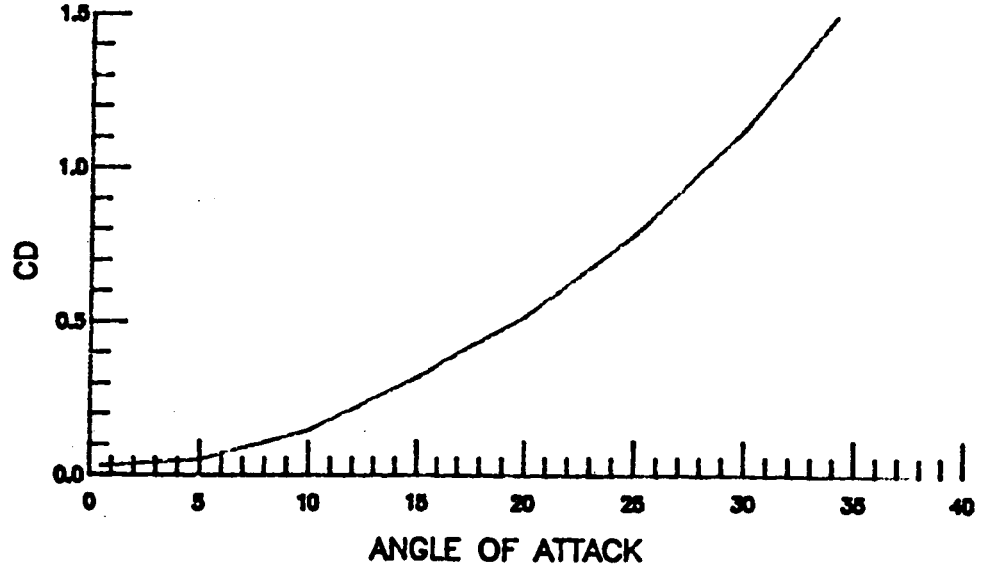

(c) CD vs

Figure 7. Continued

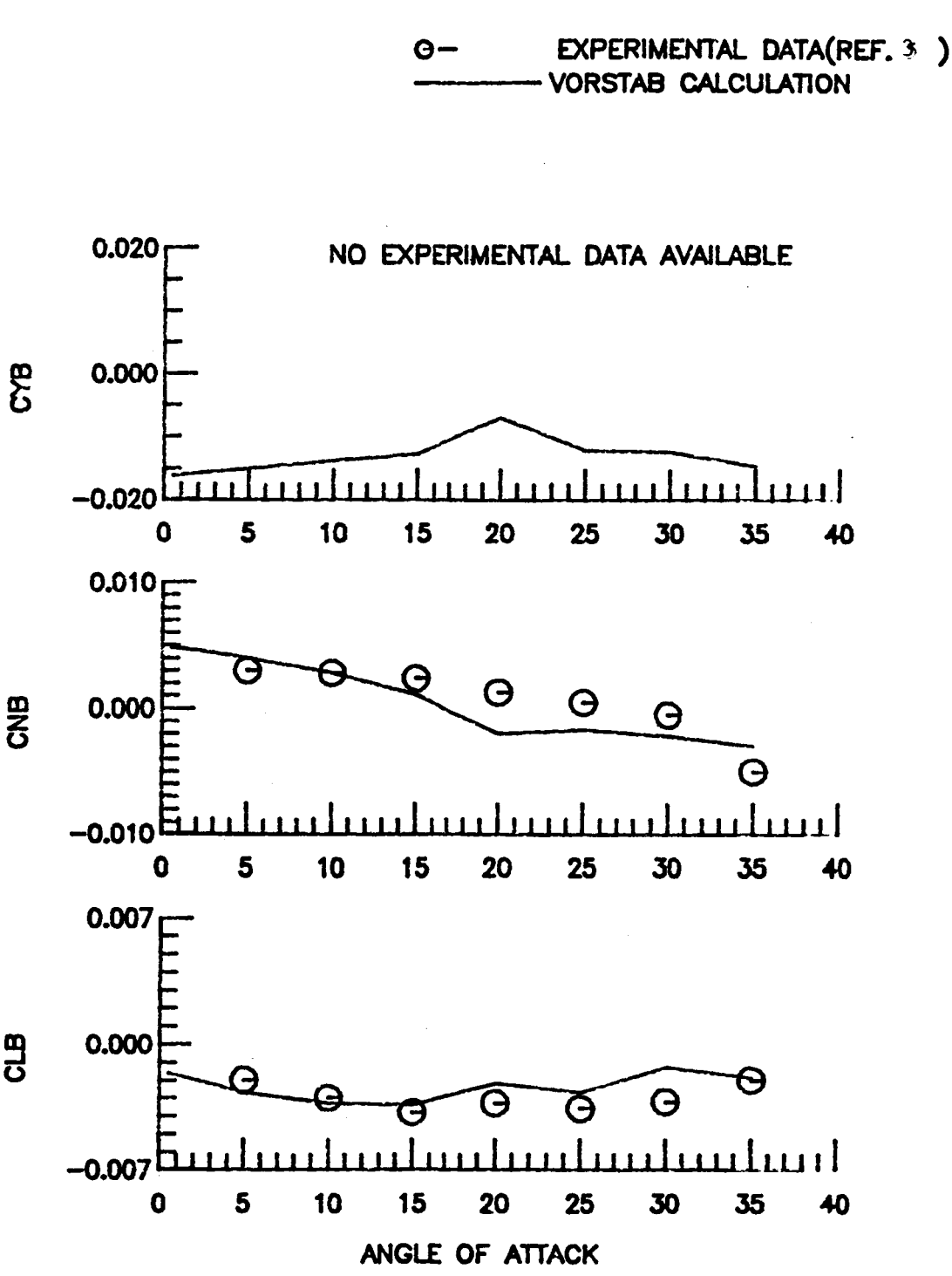

Figure 8. Lateral Derivatives Calculation Based on The Body Axis at $\beta = 4$ deg.
For an F-16 Configuration.

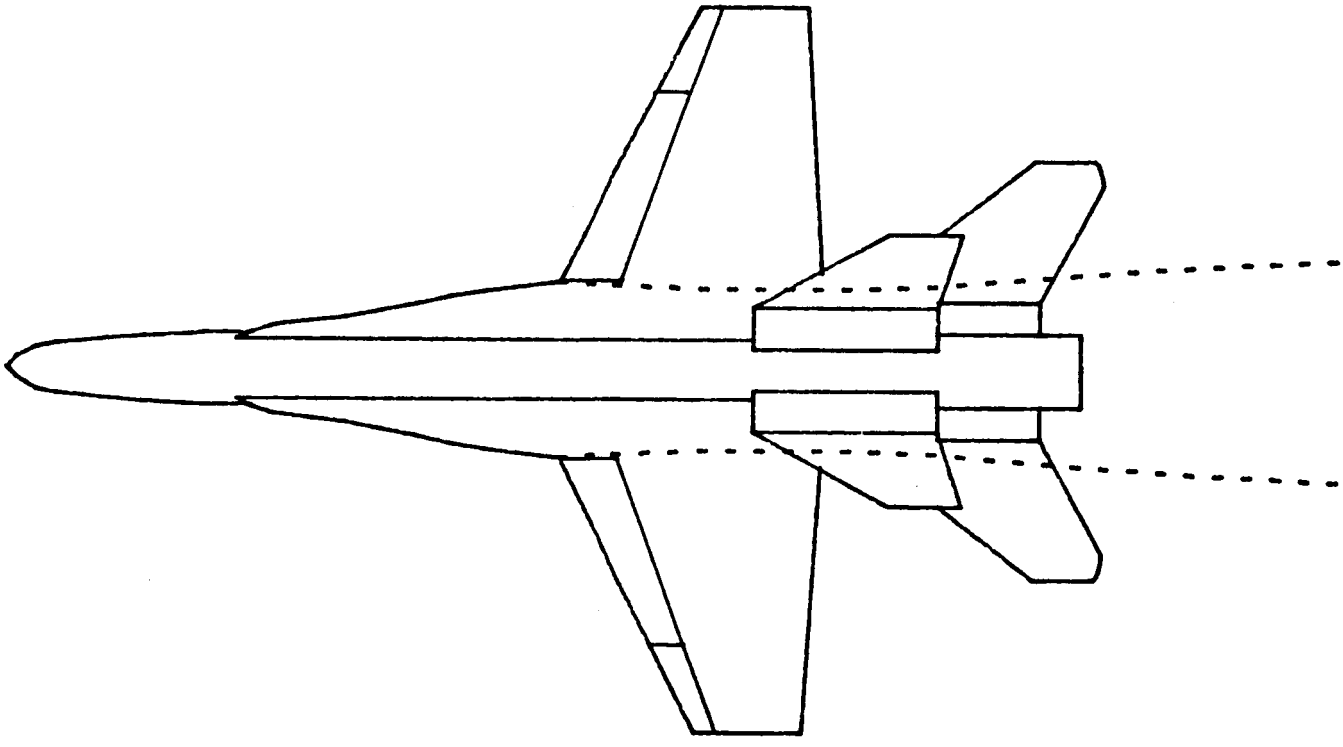

Figure 9 An F/A-18 Configuration with Leading-Edge Flaps

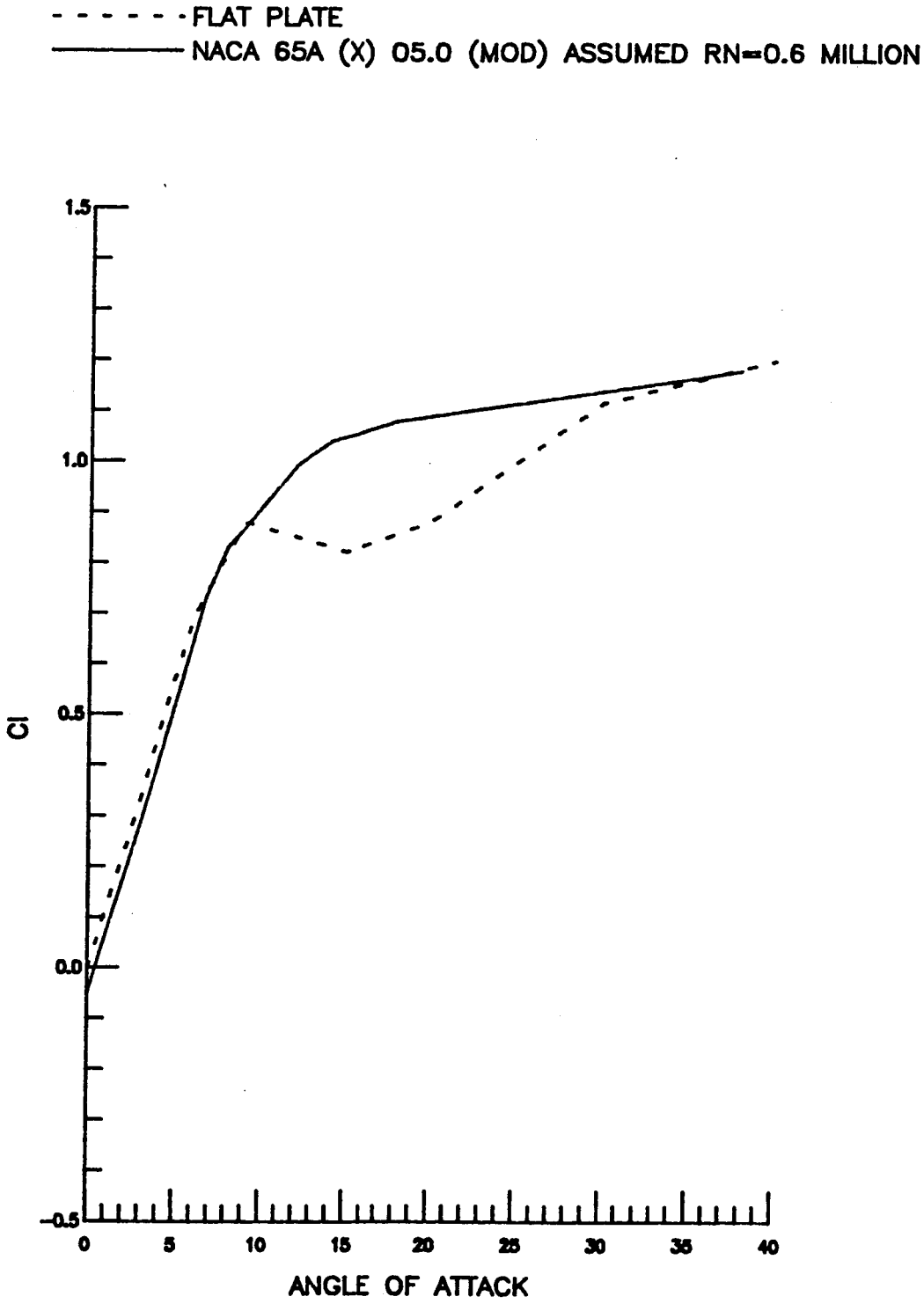

Figure 10. Sectional Data for an F-18 Configuration with Leading Edge Flap Deflection Angle = 25 deg.

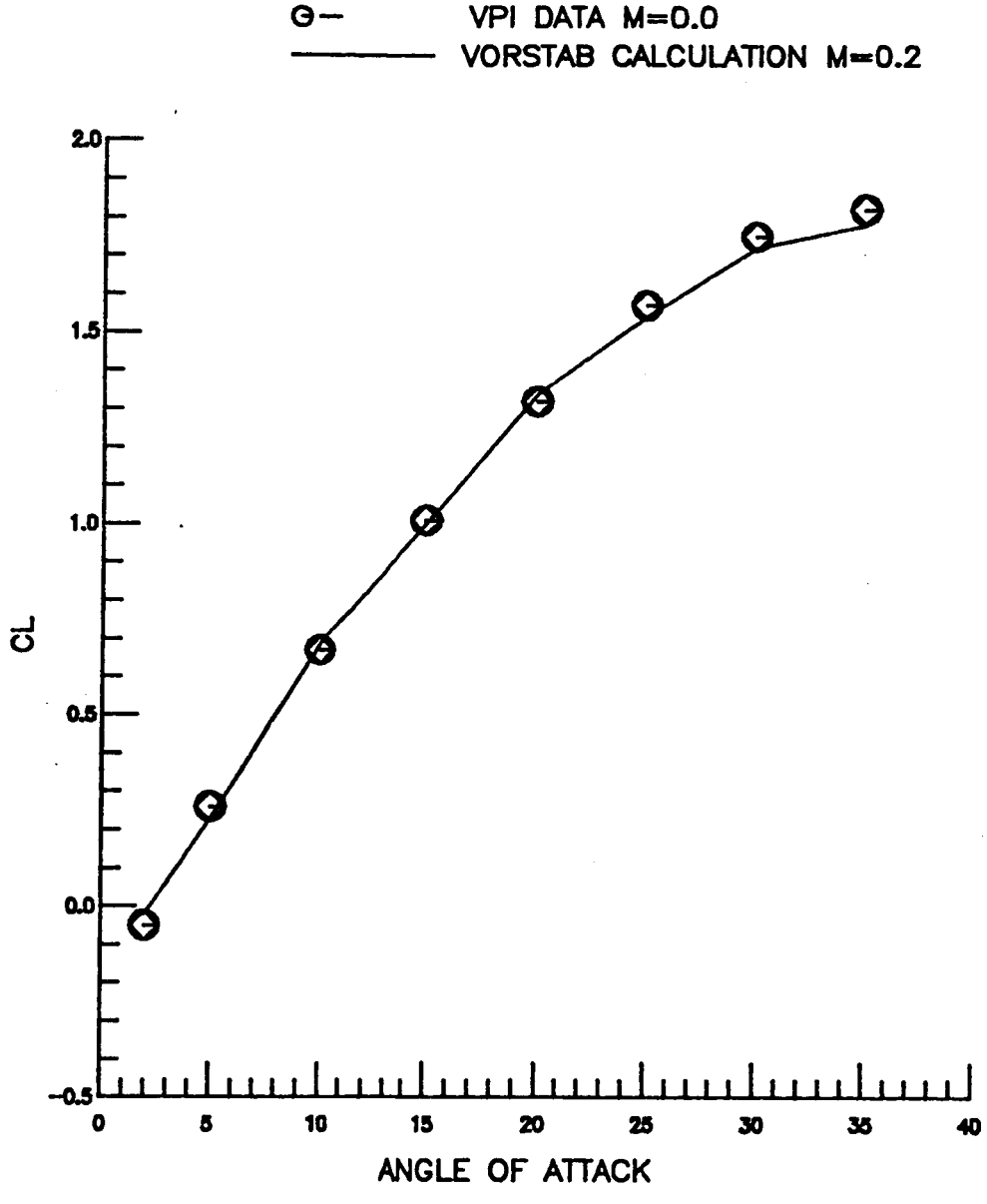

(a) CL vs

Figure 11. Longitudinal Aerodynamic Characteristics for an F-18 Configuration with $\alpha_{le} = 25°$

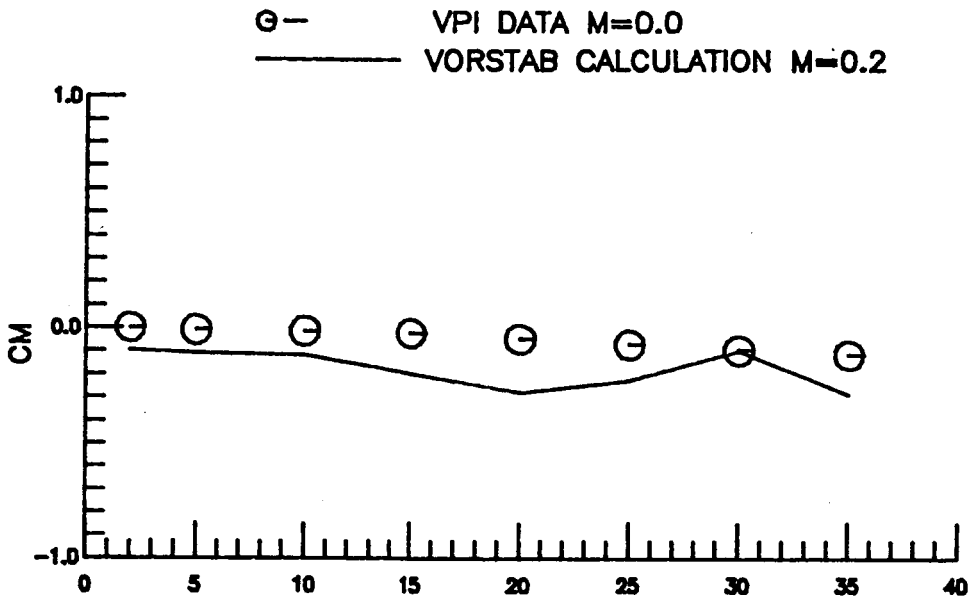

(b) CM vs

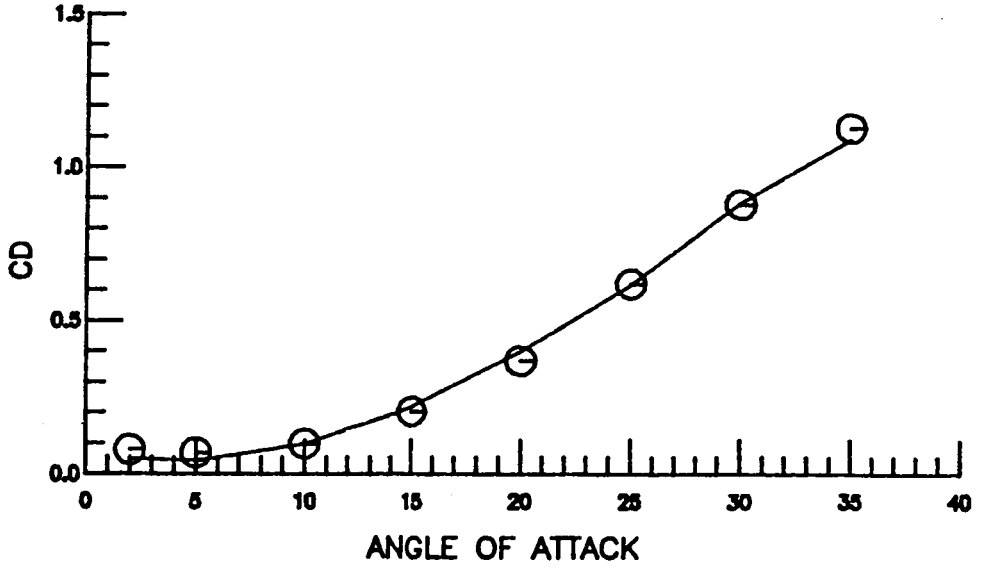

(c) CD vs

Figure 11. Continued

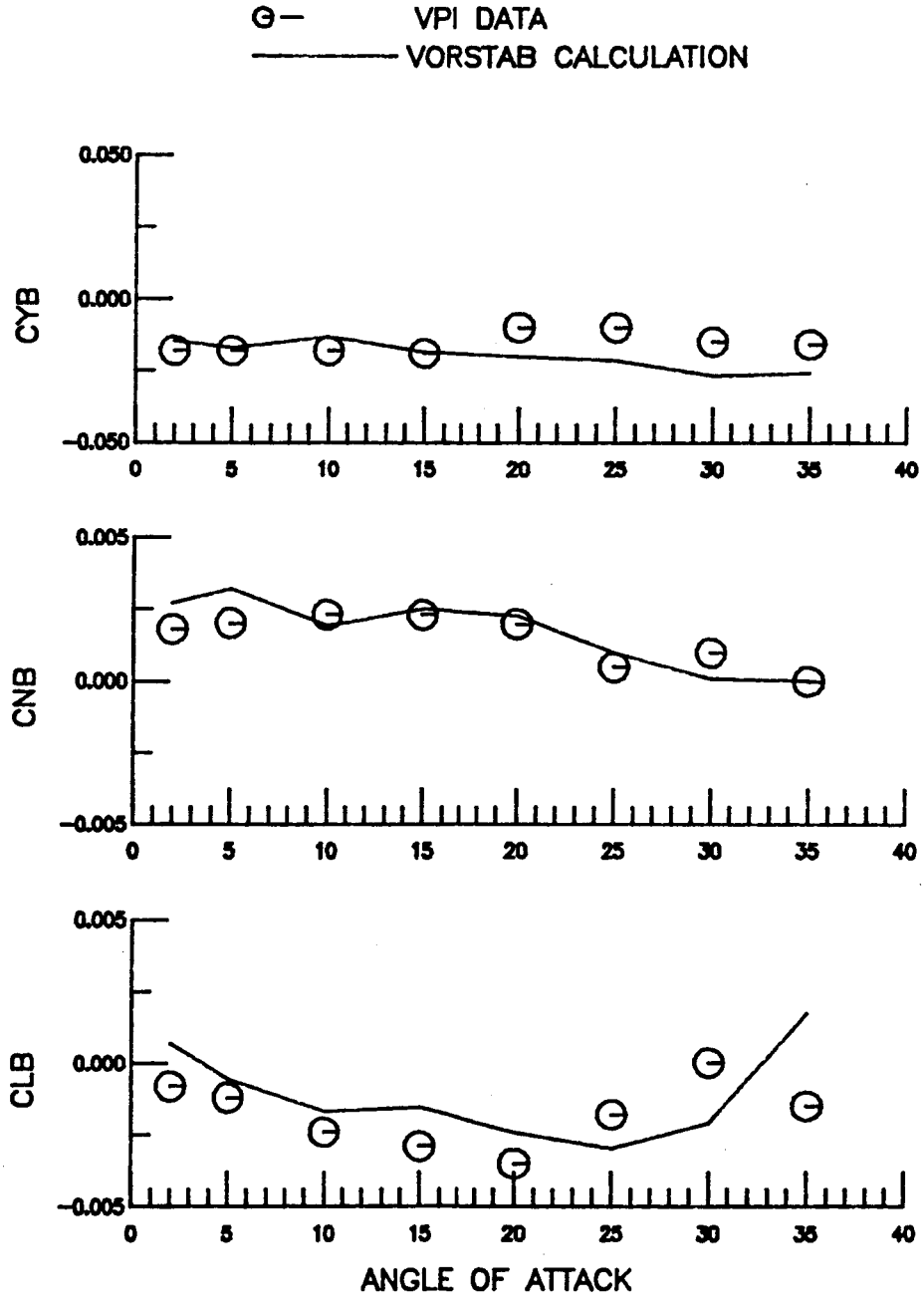

Figure 12. Lateral Derivatives Calculation Based on the Body Axis at β = 5 deg. For An F-18 Configuration.

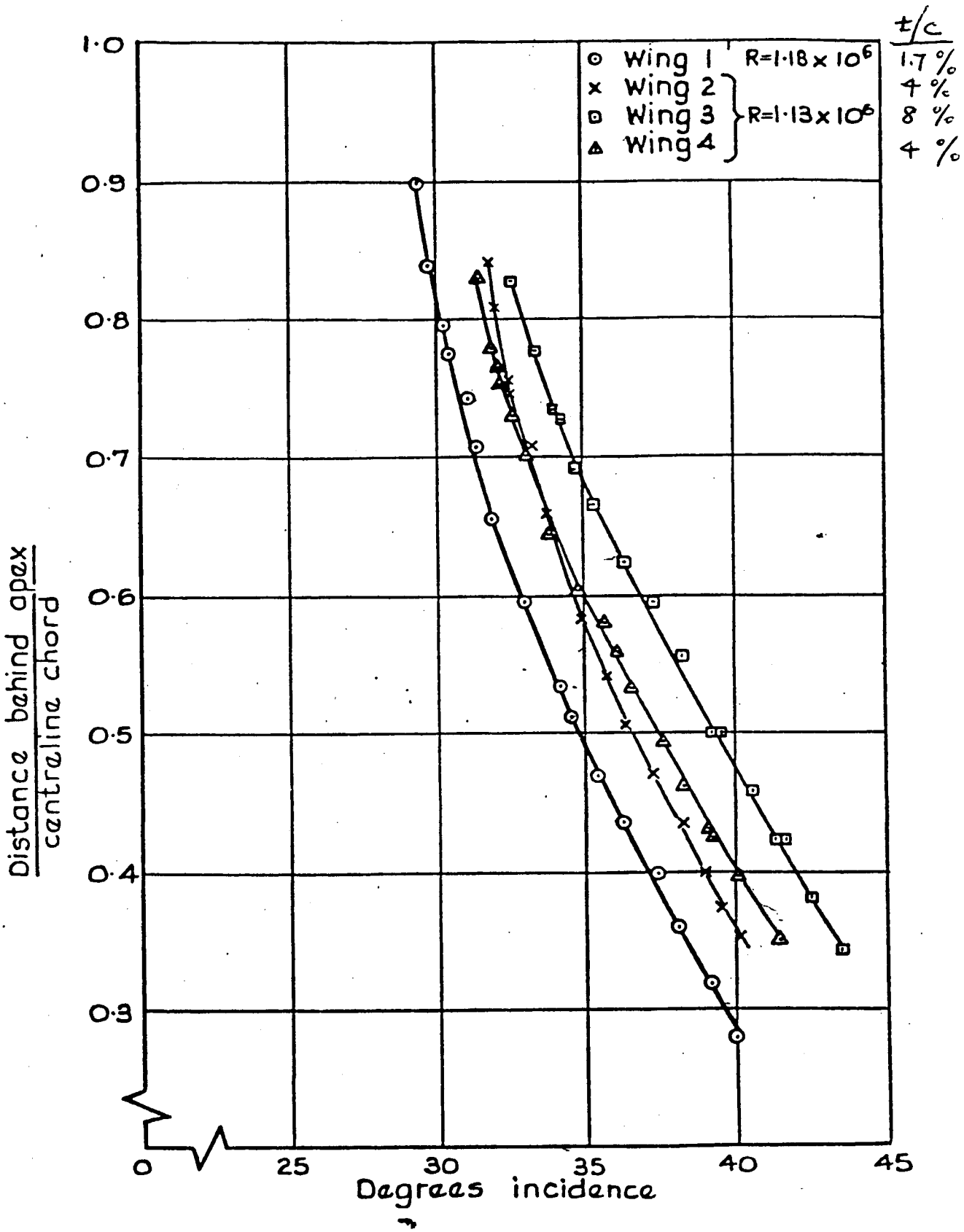

Figure 13. Influence of Thickness Distribution on Vortex Breakdown Position For a Delta Wing of 70-deg Sweep.

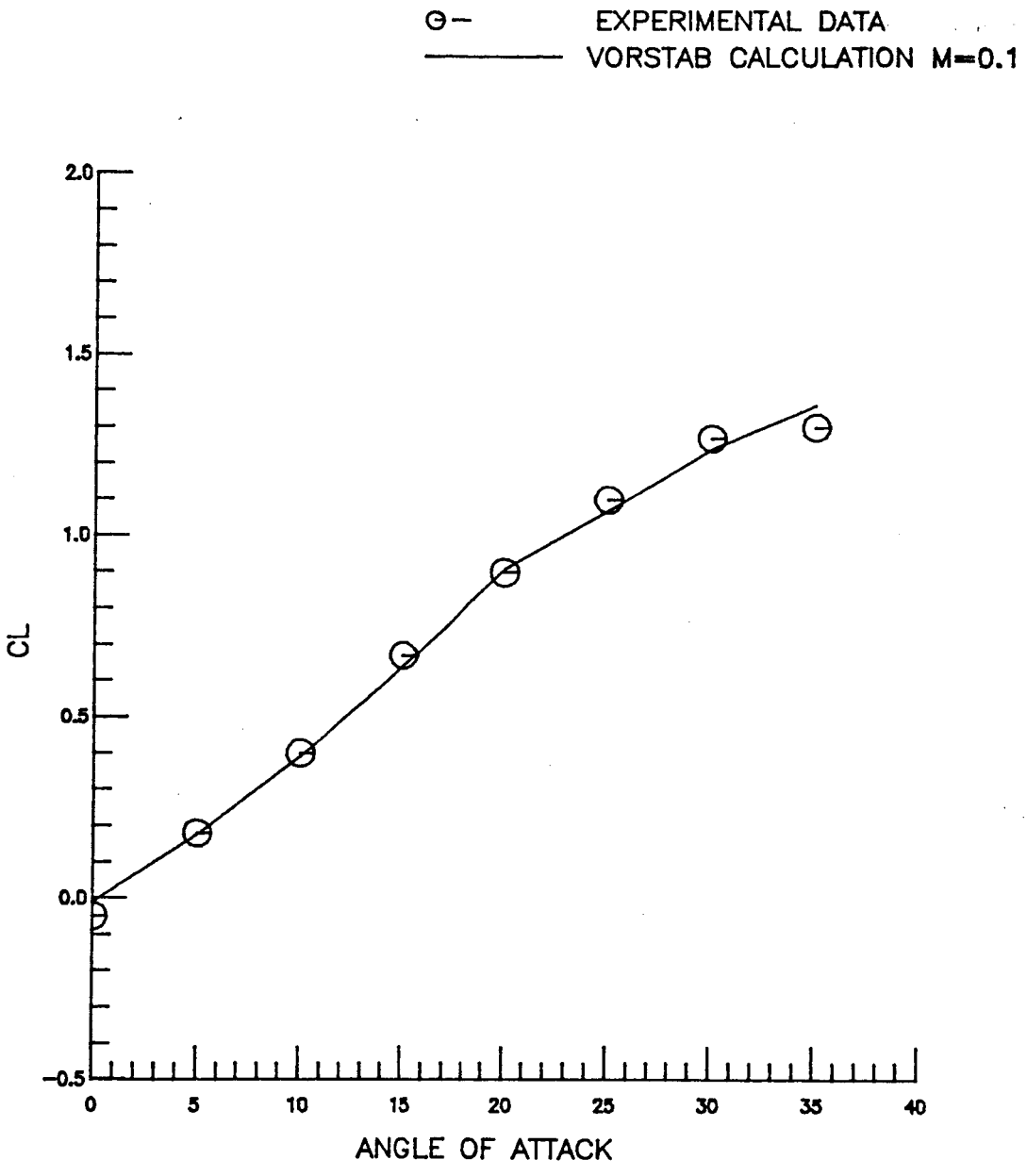

(a) CL vs

Figure 14. Longitudinal Aerodynamic Characteristics for a F-106 Configuration

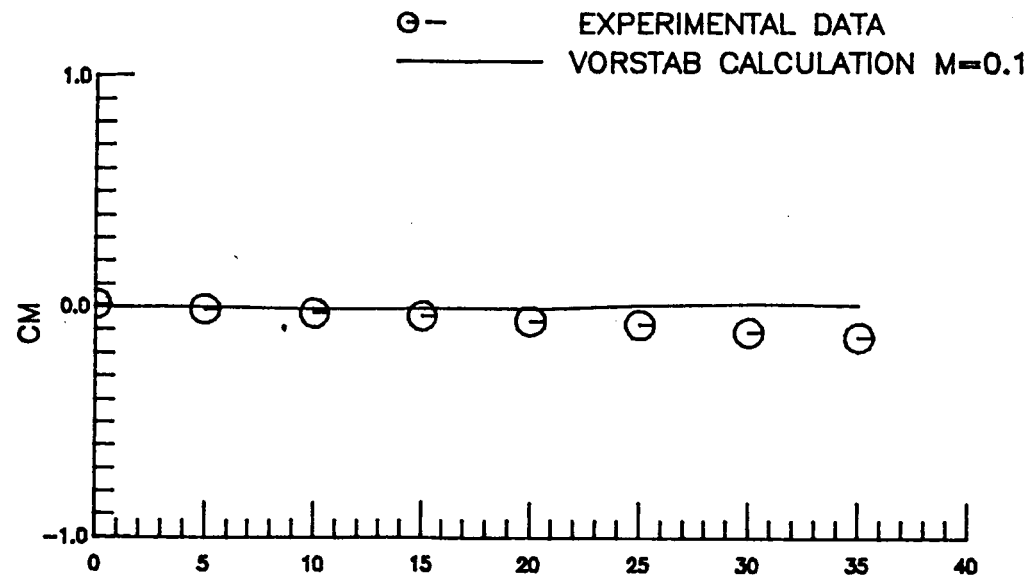

(b) CM vs

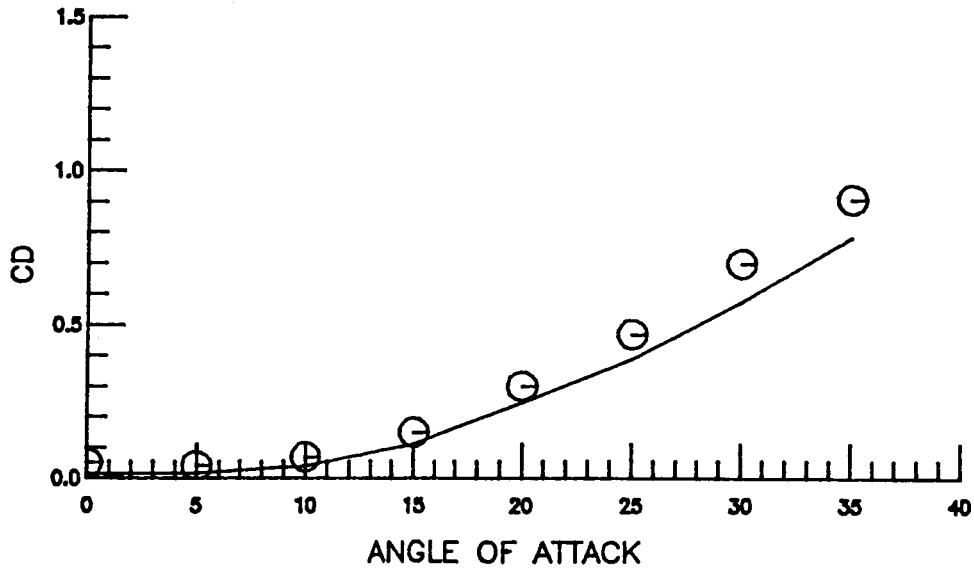

(c) CD vs

Figure 14. Continued

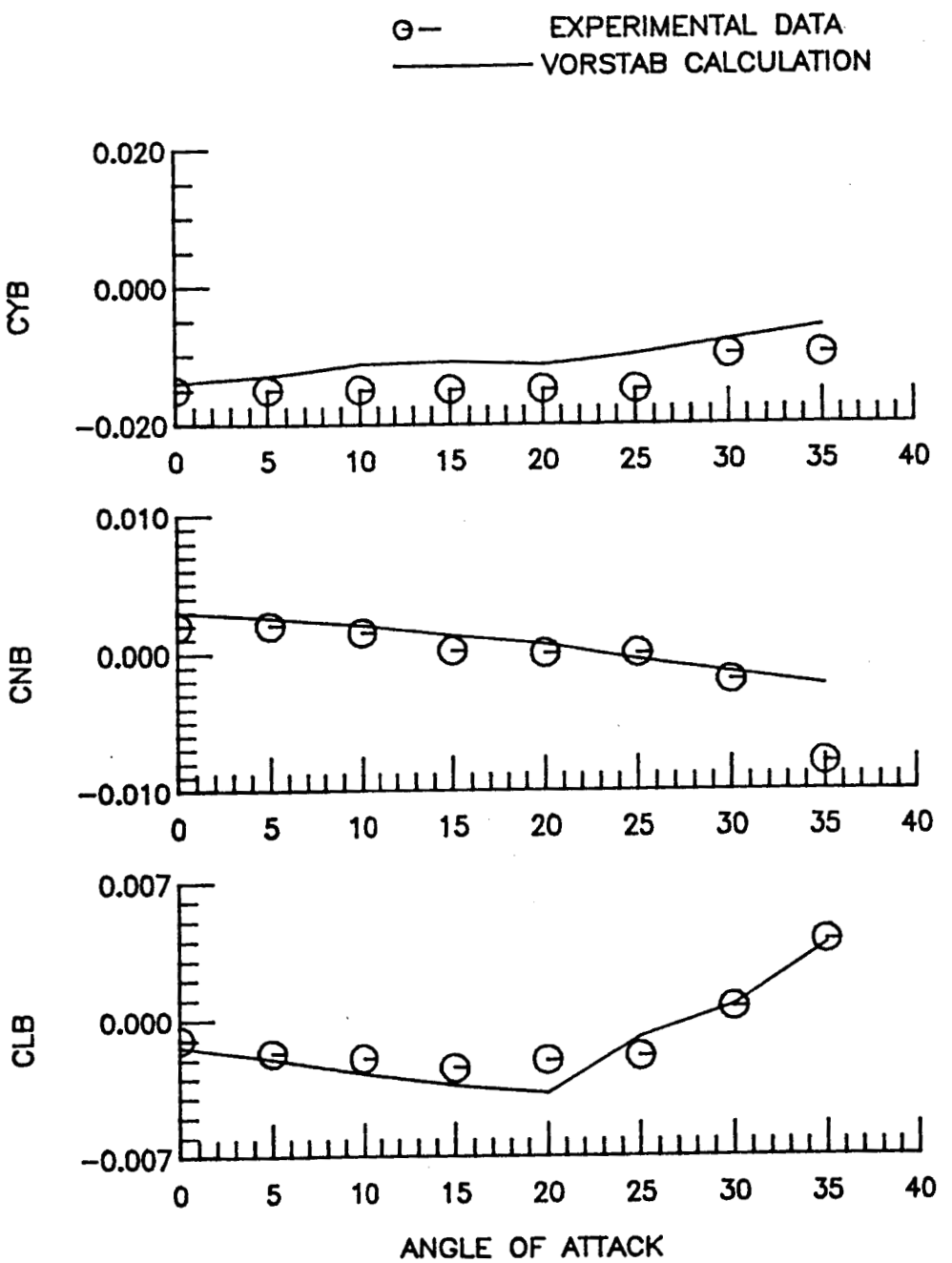

Figure 15. Lateral Derivatives Calculation Based on The Body Axis at $\beta = 5$ deg. For a Basic F-106 Configuration.